Tetrahedron
journal homepage: www.elsevier.com

Petroquinones: Trimeric and dimeric xestoquinone derivatives isolated from the marine sponge *Petrosia alfiani*

Natsuki Tanokashira [a,†], Sanako Kukita [a,†], Hikaru Kato [a,†], Tatsuo Nehira [b], Esther D. Angkouw [c], Remy E. P. Mangindaan [c], Nicole J. de Voogd [d], and Sachiko Tsukamoto [a,*]

[a] *Graduate School of Pharmaceutical Sciences, Kumamoto University, Kumamoto 862-0973, Japan*
[b] *Graduated School of Integrated Arts and Sciences, Hiroshima University, Higashi-hiroshima 739-8521, Japan*
[c] *Faculty of Fisheries and Marine Science, Sam Ratulangi University, Kampus Bahu, Manado 95115, Indonesia*
[d] *Naturalis Biodiversity Center, P.O. Box 9517, 2300 RA Leiden, The Netherlands*

ARTICLE INFO

Article history:
Received
Received in revised form
Accepted
Available online

Keywords:
Marine sponge
Petrosia alfiani
Quinone
USP7

ABSTRACT

We isolated 16 new xestoquinone derivatives, including two trimers, six dimers, and four monomers with containing thiomorpholine 1,1-dioxide and pyrrolidine-2,4-diol moieties, from the marine sponge *Petrosia alfiani* and determined their structures including the absolute configurations using computational methods. They exhibited potent inhibitory activities against USP7 with IC_{50} values in the range of 0.13–2.0 μM.

1. Introduction

Xestoquinone[1] (**17**, Fig. 1) is a pentacyclic quinone, which has been isolated from several marine sponges together with its metabolites. Notably, these compounds have been reported to exhibit a wide variety of biological properties, including cytotoxic, antimicrobial, and Na,K-ATPase inhibitory activities.[2] As part of our ongoing search for new biologically active natural products, we recently investigated the extracts of two specimens of the marine sponge *Petrosia alfiani*, which were collected from two different locations in Indonesia. The extracts of both of these sponges exhibited inhibitory activity against ubiquitin-specific protease 7 (USP7), an enzyme involved in the removal of ubiquitin from ubiquitinated target proteins including Mdm2.[3,4] Mdm2 is a ubiquitin-protein ligase (E3) for the tumor suppressor protein p53 and inhibits the activity of this protein through its direct binding. Notably, USP7 inhibitors can induce the proteasome-mediated degradation of auto-ubiquitinated Mdm2, leading to the stabilization of p53 in cells, and have consequently attracted considerable interest as potential drugs for the treatment of cancer. Herein, we report the isolation, structural determination, and biological evaluation of 16 new xestoquinone derivatives including petroquinones A–L (**1**–**12**) (Fig. 1) from the *P. alfiani*. Among these derivatives, **1** and **2** were found to be novel trimeric structures, whereas **3**–**8** were structurally diverse dimers.

2. Results

2.1. Structure elucidation

2.1.1. Petroquinones A (1) and B (2)

Petroquinones A (**1**) and B (**2**) were determined to have the same molecular formula of $C_{60}H_{36}O_{12}$ by HRESIMS. The ^{1}H and ^{13}C NMR spectra of **1** (Table 1) were similar to those of xestoquinone[1] (**17**) except for the absence of two of the CH signals belonging to the quinone moiety (i.e., H-14/C-14 and H-15/C-15 in **17**), which were replaced by two quaternary carbons (i.e., δ_C 140.4 and 140.6 in **1**). These data implied that **1** was a symmetrical *cyclo*-tri-xestoquinone. The ^{1}H and ^{13}C NMR spectra of **2** (Table 2) contained three times as many signals as those of **1**, including six additional quaternary carbons (δ_C 140.0, 140.5, 140.55, 140.59, 140.7, and 141.1), which indicated that the structure of **2** was an asymmetrical *cyclo*-tri-xestoquinone. Biogenetic considerations suggested that **1** and **2** would adopt 6*S*,6'*S*,6"*S* configurations. Density functional theory (DFT) calculations were conducted to determine the energy-minimized conformation of **1**. The results of this calculation revealed that **1** would adopt a twisted three-bladed propeller-like structure to minimize steric crowding between the quinone moieties (Fig. 2a). In contrast to **17** ($[\alpha]_D$ +22 (*c* 0.1, CH_3CN)) and **2** ($[\alpha]_D$ -6 (*c* 0.1,

* Corresponding author. Tel./fax: +96 371 4380; e-mail: sachiko@kumamoto-u.ac.jp (S. Tsukamoto).

† These authors equally contributed.

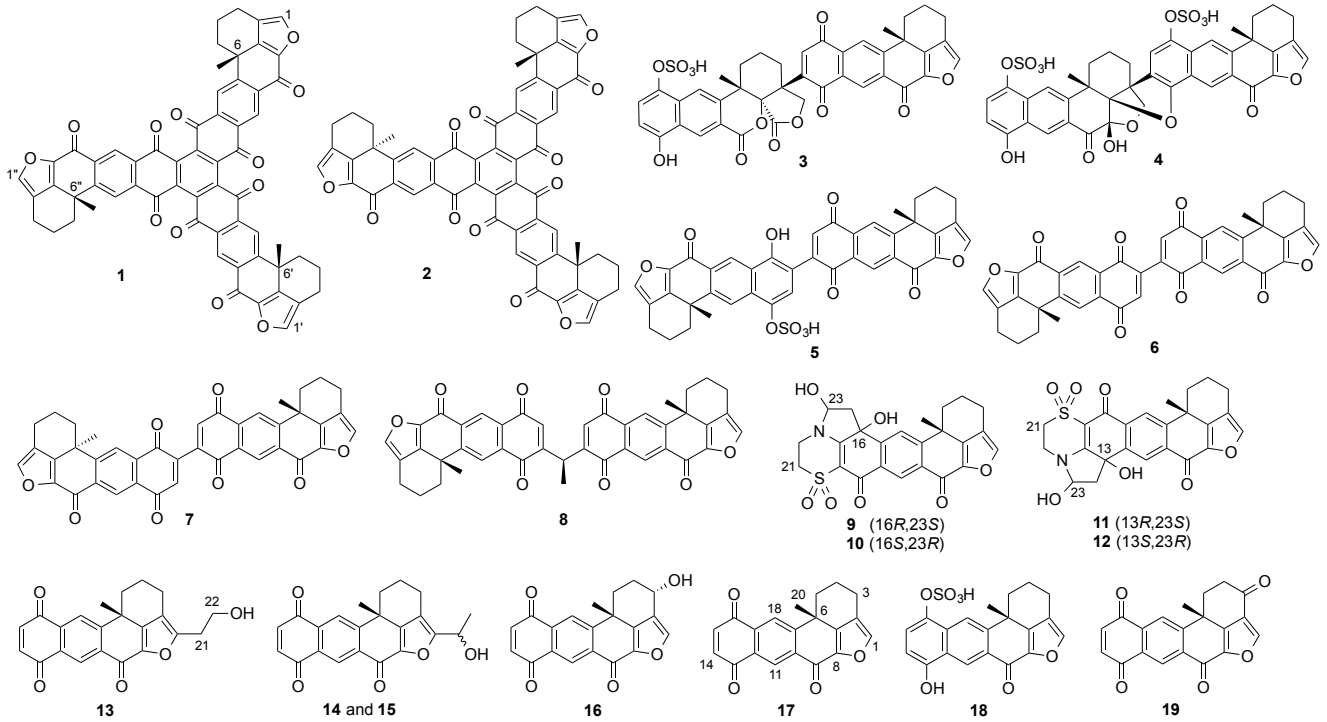

Fig. 1. Structures of compounds **1–19**.

Table 1
^{1}H and ^{13}C NMR data of **1** in $CDCl_3$

No.	δ_C [b]	δ_H, mult	HMBC	No.	δ_C [b]	δ_H, mult	HMBC
1	145.0	7.49, br s	2, 7, 8	10	138.5		
2	121.8			11	127.6	8.99, s	
3	17.0	2.71, m	2, 4	12	132.5		
		2.90, m	2, 4	13	181.1		
4	18.5	2.30, m	3	14	140.4 [a]		
		2.33, m	3	15	140.6 [a]		
5	31.0	1.94, m	6, 7	16	181.8		
		2.63, m	6, 7	17	135.7		
6	37.6			18	124.0	8.31, br s	6, 10, 12, 16
7	147.6			19	157.0		
8	143.9			20	33.1	1.54, s	5, 6, 7, 19
9	169.7						

[a] May be interchangeable.
[b] The carbon chemical shifts of C-1'-C-20' and C-1"-C-20" are same as those of C-1─C-20.

Table 2
^{1}H and ^{13}C NMR data of **2** in $CDCl_3$

No.	δ_C	δ_H,	HMBC	No.	δ_C	δ_H, mult	HMBC
1	145.0	7.54, s	2, 7, 8	10'	138.5		
2	121.5			11'	127.5	9.02, s	9', 13', 17', 19'
3	17.0	2.72, m	2, 4, 7	12'	132.5		
		2.90, m	2, 4, 7	13'	180.8		
4	18.5	2.19, m		14'	140.5		
		2.31, m		15'	140.7[a]		
5	31.4	1.82, m	6	16'	181.8[a]		
		2.55, m	3	17'	135.7		
6	37.5			18'	124.1	8.31, s	6', 10', 12', 16'
7	147.0			19'	156.8		
8	144.1			20'	33.1	1.54, s	5', 6', 7', 19'
9	169.8			1"	144.7	7.38, s	2", 7", 8"
10	138.8			2"	121.7		
11	127.7	9.04, s	9, 13, 17, 19	3"	17.0	2.72, m	2", 4", 7"
12	132.8					2.87, m	2", 4", 7"
13	180.9			4"	18.5	2.27, m	
14	140.0[a]					2.30, m	
15	140.55			5"	31.1	1.93, m	6"
16	182.3[a]					2.61, m	3"
17	135.7			6"	37.5		
18	123.8	8.31, s	6, 10, 12, 16	7"	147.3		
19	156.8			8"	143.9		
20	32.7	1.64, s	5, 6, 7, 19	9"	169.6		
1'	145.0	7.50, s	2', 7', 8'	10"	138.5		
2'	121.7			11"	127.6	9.00, s	9", 13", 17", 19"
3'	16.9	2.72, m	2', 4', 7'	12"	132.4		
		2.87, m	2', 4', 7'	13"	180.6		
4'	18.5	2.27, m		14"	140.5		
		2.30, m		15"	141.1[a]		
5'	31.1	1.93, m	6'	16"	181.8[a]		
		2.61, m	3'	17"	135.7		
6'	37.5			18"	123.9	8.30, s	6", 10", 12", 16"
7'	147.3			19"	156.9		
8'	143.9			20"	32.9	1.53, s	5", 6", 7", 19"
9'	169.5						

[a] May be interchangeable.

CH_3CN)), **1** showed a large absolute optical rotation value of +389 (*c* 0.1, CH_3CN). Compound **1** also showed strong ECD intensities (Fig. 2b). These large values were attributed to **1** being a C_3-symmetric helical molecule.

2.1.2. Petroquinone C (3)

The molecular formula of petroquinone C (**3**) was determined to be $C_{40}H_{30}O_{13}S$ by HRFABMS, which indicated the presence of a sulfate moiety. The ^{1}H and ^{13}C NMR spectra of **3** (Table 3) revealed the presence of **17** (unit ***a***, Fig. 3a) bearing a substituent at the C-14 position. Consideration of the 2D NMR spectra of **3** indicated that unit ***b*** contained two carbonyl carbons (δ_C 170.4 (C-8')) and 162.4 (C-9')), two oxygen-bearing carbons (δ_C 73.7 (C-1') and 87.3 (C-7')), and a monosulfated naphthalene-1,4-diol moiety (Fig. 3a). Comprehensive analysis of these 2D NMR data revealed that unit ***b*** of **3** contained a γ-lactone ring rather than the furan ring found in **17** and that the remaining oxygen atom was located between the C-7' and C-9' positions as part of a δ-lactone ring. HMBC analysis revealed the presence of correlations from H-15 (δ_H 7.57) to C-2' (δ_C 49.6) and from H-1' (δ_H 4.68) to C-14 (δ_C 146.3), which clearly showed that C-2' (unit ***b***) was connected to C-14 (unit ***a***). The absolute configurations at C-6 and C-6' were determined to be *S* based on the biogenetic relationship between **3** and **17**. An NOE correlation was

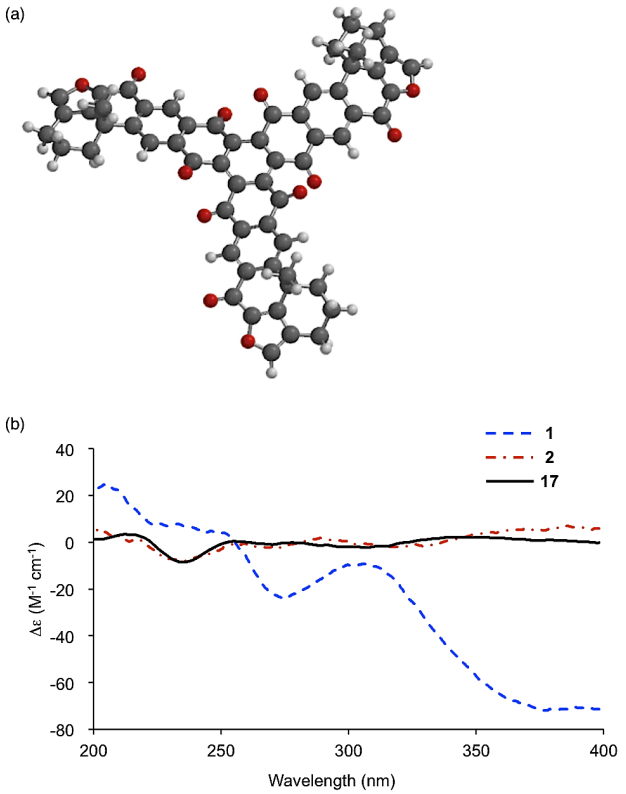

Fig. 2. (a) Energy-minimized structure of **1**. (b) ECD spectra of **1**, **2**, and **17**.

Table 3.
^{1}H and ^{13}C NMR data of **3** in DMSO-d_6

No.	δ_C	δ_H, mult	HMBC	No.	δ_C	δ_H, mult (J in Hz)	HMBC
1	146.3	8.00, s	7, 8	1’	73.7	4.59, d (6.0) 4.68, d (6.0)	2’, 3’, 7’, 8’ 3’, 14
2	121.7			2’	49.6		
3	16.2	2.60, m 2.84, m	2, 7 2, 5, 7	3’	31.8	1.60, m 2.99, m	
4	17.8	2.06, m 2.22, m		4’	17.7	1.78, m 1.92, m	
5	30.4	1.60, m 2.68, m		5’	31.3	1.78, m 2.39, m	
6	38.3			6’	38.3		
7	148.0			7’	87.3		
8	143.0			8’	170.4		
9	169.4			9’	162.4		
10	137.0			10’	119.5		
11	125.8	8.76, s	9, 13, 17, 19	11’	126.5	8.74, s	9’, 13’, 17’, 19’
12	131.7			12’	122.6		
13	184.1			13’	150.6		
14	146.3			14’	108.1	6.83, d (6.0)	12’, 13’, 16’
15	140.3	7.57, s	13, 14, 17, 2’	15’	121.4	7.41, d (6.0)	13’, 16’, 17’
16	183.9			16’	141.3		
17	132.5			17’	131.1		
18	122.5	8.27, s	6, 10, 12, 16	18’	116.2	7.97, s	6’, 10’, 12’, 16’
19	155.8			19’	143.0		
20	31.6	1.51, s	5, 6, 7, 19	20’	28.5	1.45, s	5’, 6’, 7’, 19’
				OH-13’		10.33, s	12’, 13’

observed between H-15 (δ_H 7.57) and H_3-20’, which was consistent with the 2’*S* configuration (Fig. 3b). NOE correlations were also observed between H-18’ (δ_H 7.97) and H_2-5’ (δ_H 1.78 and 2.39). Calculated distances between H-18’ and H_2-5 for 7’*S*-**3** and 7’*R*-**3** were 2.39/2.34 (α/β) and 4.42/3.80 (α/β) Å, respectively. Furthermore, those between H-20’ and H-15 for 7’*S*-**3** and 7’*R*-**3** were 2.16 and 2.15 Å, respectively. These data allowed for the unambiguous assignment of the 7’*S* configuration. The structure of **3** was therefore determined to be as shown in the Fig. 3.

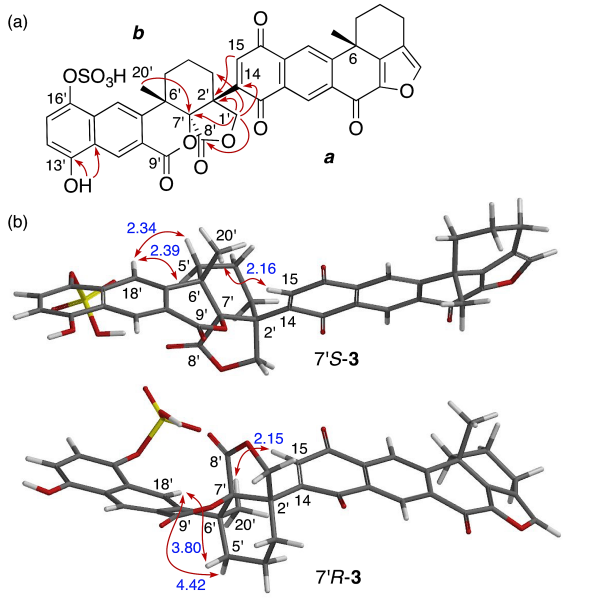

Fig. 3. (a) Key HMBC correlations for **3**. (b) Calculated distances (Å) between two selected protons for 7’*S*-**3** and 7’*R*-**3**.

2.1.3. Petroquinone D (4)

ESIMS analysis of petroquinone D (**4**) in the negative ionization mode revealed the presence of an intense peak with an *m/z* value of 407, along with a weak peak with an *m/z* value of 815, which indicated that the former of these two peaks was a divalent ion peak. HRESIMS analysis of **4** gave a peak with an *m/z* value of 407.0531 for $[M–2H]^{2–}$, which was consistent with the molecular formula of $C_{40}H_{32}O_{15}S_2$, indicating the presence of two sulfates. Analysis of 2D NMR spectra (Table 4) suggested that **4** was a derivative of dimeric xestoquinol sulfate (**18**). The unit ***b*** of **4** contained a tetrahydrofuran moiety (C-1’ (δ_C 77.0, CH_2), C-2’ (δ_C 57.5, C), C-7’ (δ_C 97.5, C), and C-8’ (δ_C 102.9, C)) instead of the furan ring found in **18**. An exchangeable proton was observed at δ_H 7.35 (OH-8’), which showed correlations with the C-7’, C-8’, and C-9’ positions by HMBC analysis (Fig. 4a), indicating the presence of a hydroxyl group at C-8’. HMBC analysis also revealed correlations between H_2-1’ (δ_H 3.19 and 3.87)/C-14 (δ_C 125.1), H-3’ (δ_H 1.82)/C-14, and H-15 (δ_H 7.39)/C- 2’, which indicated a connection between C-2’ and C-14 (Fig. 4a). A phenolic hydrogen atom was observed at δ_H 10.38 (OH-13’), which showed correlations to the C-12’ (δ_C 123.8) and C-13’ (δ_C 151.8) positions by HMBC, indicating the presence of a phenol group at C-13’. The remaining oxygen atom formed an ether linkage between two carbons among C-7’, C-13 (δ_C 152.2), C-16 (δ_C 144.0), and C-16’ (δ_C 141.6). Among these carbons, it was only possible for C-13 and C-7’ to form an ether linkage based on their respective distances (Fig. 4b). The chemical shifts of C-16 and C-16’ were higher than those of C-13 and C-13’ (δ_C 151.8), which suggested that the sulfate groups were positioned at C-16 and C-16’. Biogenetic consideration suggested that **4** would adopt a 6*S*,6’*S*-configuration. Furthermore, NOE correlations from H-11 to H_3-20’ and OH-8’ indicated that the absolute configurations of C-2’, C-7’, and C-8’ were consistent with those shown in Fig. 4b. Chemical shift calculations were conducted for the 8’*R* and 8’*S* isomers. The averaged derivation of the carbons in the two rings substituted with OH-8’ were 4.9 and 1.6 ppm for 8’*R* and 8’*S*, respectively (Fig. 4c), which showed that the 8’*S* isomer was favored over the 8’*R* isomer. The structure of **4** was therefore established together with its absolute configuration.

Table 4
^{1}H and ^{13}C NMR data of **4** in DMSO-d_6

No.	δ_C	δ_H, mult (*J* in Hz)	HMBC	No.	δ_C	δ_H, mult (*J* in Hz)	HMBC
1	145.7	7.92, s	2, 7, 8	1’	77.0	3.19, d (6.0)	15, 3’
						3.87, d (6.0)	15, 2’, 7’, 8’
2	121.9			2’	57.5		
3	17.1	2.62, m	1, 2, 4, 7	3’	25.9	0.87, m	
		2.85, m	1, 2, 4, 5, 7			1.82, m	14, 2’, 5’, 7’
4	18.6	2.11, m		4’	15.8	1.19, m	
		2.24, m				1.84, m	
5	32.2	1.73, m		5’	26.2	1.64, m	19’
		2.52, m				2.24, m	7’
6	36.4			6’	40.7		
7	147.5			7’	97.5		
8	144.2			8’	102.9		
9	171.8			9’	195.1		
10	131.2			10’	127.4		
11	123.4	8.91, s	9, 13, 17, 19	11’	124.2	8.72, s	9’, 13’, 17’, 19’
12	117.9			12’	123.8		
13	152.2			13’	151.8		
14	125.1			14’	108.4	6.83, d (6.0)	12’, 13’, 16’
15	115.7	7.39, s	13, 16, 17, 2’	15’	122.6	7.33, d (6.0)	13’, 16’, 17’
16	144.0			16’	141.6		
17	129.3			17’	132.4		
18	120.3	8.34, s	6, 10, 12, 16	18’	119.9	8.28, s	6’, 10’, 12’, 16’
19	146.0			19’	142.2		
20	36.4	1.49, s	5, 6, 7, 19	20’	30.8	1.43, s	5’, 6’, 7’, 19’
				OH-8’		7.35, s	7’, 8’, 9’
				OH-13’		10.38, s	12’, 13’

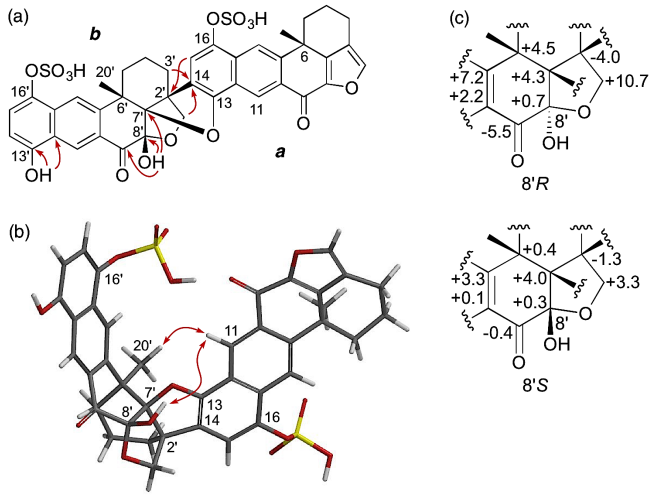

Fig. 4. (a) Key HMBC correlations for **4**. (b) Key NOE correlations for **4**. (c) Deviations in the calculated ^{13}C chemical shifts from the experimental data for 8’*R* and 8’*S* isomers of **4**.

2.1.4. Petroquinones E-G (5-7)

The molecular formula of petroquinone E (**5**) was determined to $C_{40}H_{28}O_{11}S$ by HRESIMS, and its structure was determined by NMR analysis (Table 5). HRESIMS analysis revealed that the molecular formula for petroquinones F (**6**) and G (**7**) was $C_{40}H_{26}O_8$, which indicated that these compounds shared dimeric features. The ^{1}H NMR spectrum of **6** revealed the presence of 13 hydrogen atoms (Table 6), which suggested this compound had a C_2-symmetrical structure. HMBC analysis of **6** (Fig. 5a) confirmed that the monomeric units were connected by a single C–C bond between C-14 and C-14’. In contrast, the ^{1}H NMR spectrum of **7** showed that there were slight differences in the respective aromatic hydrogen atoms of the two different monomer units ***a*** and ***b***: δ 9.10/9.08 (H-11/H-11’), 7.21/7.13 (H-15/H-14’), and 8.29/8.27 (H-18/H-18’) (Table 6). HMBC analysis of **7** clearly showed that the two different monomer units ***a*** and ***b*** were joined together through a single C–C bond between C-14 and C-15’ (Fig. 5a). In the presence of quinolone and acetic acid, xestoquinone (**17**) underwent a dimerization reaction to give **6** in 7% yield. The ECD spectra of natural and semisynthetic **6** showed identical curves (Fig. 5b), which confirmed the 6*S* configuration of **6** together with biogenetic considerations.

Table 5
^{1}H and ^{13}C NMR data of **5** in DMSO-d_6

No.	δ_C	δ_H, mult	HMBC	No.	δ_C	δ_H, mult	HMBC
1	146.2	8.01, s	2, 7, 8	1’	145.2	7.92, s	2’, 7’, 8’
2	121.7			2’	121.4		
3	16.3[a]	2.63, m	2	3’	16.6[a]	2.63, m	2’
		2.85, m	2			2.85, m	2’
4	17.9[b]	2.09, m		4’	18.1[b]	2.09, m	
		2.24, m				2.24, m	
5	30.4	1.65, m		5’	31.3	1.75, m	
		2.70, m				2.53, m	
6	37.1			6’	35.9		
7	148.0			7’	146.9		
8	143.1			8’	143.7		
9	169.6			9’	171.3		
10	136.9			10’	131.0		
11	125.5	8.80, s	9, 13, 17, 19	11’	123.9	9.10, s	9’, 13’, 17’, 19’
12	130.6			12’	123.8		
13	182.3			13’	147.9		
14	148.2			14’	115.0		
15	137.6	7.14, s	13, 17, 14’	15’	121.5	7.39, s	13’, 16’, 17’, 14
16	184.2			16’	141.2		
17	133.4			17’	130.2		
18	122.7	8.33, s	6, 10, 12, 16	18’	119.2	8.32, s	6’, 10’, 12’, 16’
19	155.8			19’	146.7		
20	31.3	1.54, s	5, 6, 7, 19	20’	33.5	1.48, s	5’, 6’, 7’
				OH-13’		9.89, s	12’

[a, b] May be interchangeable.

Table 6
^{1}H and ^{13}C NMR data of **6** and **7** in $CDCl_3$

	6			**7**		
No.	δ_C	δ_H, mult	HMBC	δ_C	δ_H, mult	HMBC
1	145.3	7.54, s	2, 7, 8	145.1	7.54, s	2, 7, 8
2	122.0			121.5		
3	17.0	2.65, m	2	16.9	2.65, m	2, 4, 7
		2.88, m	2, 4		2.87, m	2, 4, 5, 7
4	18.3	2.20, m		18.4	2.19, m	
		2.28, m			2.28, m	
5	31.4	1.77, m	4, 7	31.2	1.76, m	
		2.60, m			2.58, m	
6	38.0			37.4		
7	147.3			147.3		
8	144.6			144.4		
9	170.7			170.0		
10	139.1			138.3		
11	127.8	9.08, s	9, 13, 17, 19	127.7	9.10, s	9, 13, 17, 19
12	130.6			130.4		
13	182.0			181.7		
14	143.8			143.6		
15	138.1	7.14, s	13, 14, 14’, 17	137.6	7.21, s	13, 14, 14’, 17
16	184.4			183.8		
17	133.8			133.3		
18	123.4	8.27, s	10, 12, 16, 19	123.2	8.29, s	10, 12, 16, 19
19	157.3			156.5		
20	32.7	1.54, s	5, 6, 7, 19	32.6	1.54, s	5, 6, 7, 19
1’				145.1	7.54, s	2’, 7’, 8’
2’				121.5		
3’				16.9	2.65, m	2’, 4’, 7’
					2.87, m	2’, 4’, 7’
4’				18.4	2.19, m	
					2.28, m	
5’				31.2	1.76, m	
					2.58, m	
6’				37.4		
7’				147.3		
8’				144.0		
9’				170.1		
10’				138.1		
11’				127.1	9.08, s	9’, 13’, 17’, 19’
12’				130.3		
13’				182.9		
14’				138.3	7.13, s	13’, 14, 14’, 17’
15’				144.3		
16’				182.5		
17’				133.3		
18’				123.9	8.27, s	10’, 12’, 16’, 19’
19’				156.6		
20’				32.6	1.54, s	5’, 6’, 7’, 19’

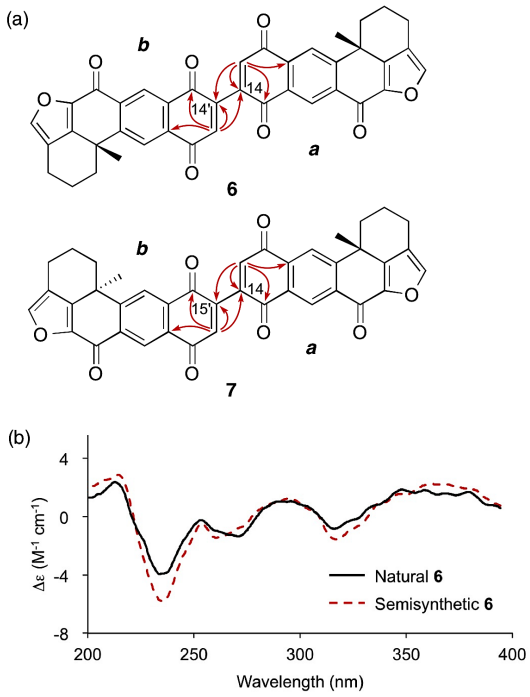

Fig. 5. (a) Key HMBC correlations for **6** and **7**. (b) ECD spectra of natural and semisynthetic **6**.

2.1.5. Petroquinone H (8)

The molecular formula of petroquinone H (**8**) was determined to be $C_{42}H_{30}O_8$ by HRESIMS, representing a C_2H_4 unit more than that of petroquinones F (**6**) and G (**7**). The NMR spectra of **8** (Table 7) revealed that it consisted of two molecules of **17**, which were linked together through an ethylidene group (δ_H 4.73 (q, J = 6.9 Hz), δ_C 31.9 (C-21); δ_H 1.48 (d, J = 6.9 Hz), δ_C 17.9 (C-22)) at the C-14 and C-15' positions, which was confirmed by HMBC analysis (Fig. 6a). Biogenetic considerations suggested that **8** existed in the 6*S*,6'*S*-configuration. To determine the configuration of C-21, we conducted ECD calculations using 21*S*- and 21*R*-**8** (Fig. 6b). Two distinct differences were observed between the ECD spectra of **8** and xestoquinone (**17**), including the negative and positive Cotton effects observed at 275 and 300 nm, respectively, which were observed in the calculated spectrum of 21*S*-**8** but not in that of 21*R*-**8**. These results show that the calculated spectrum of 21*S*-**8** was more consistent with the experimental spectrum of **8** than that of 21*R*-**8**, and the absolute configuration of **8** was therefore concluded to be 6*S*,21*S*,6'*S*.

2.1.6. Petroquinones I-L (9-12)

The molecular formula of petroquinones I–L (**9**–**12**) was determined to be $C_{24}H_{21}NO_7S$ by HRFABMS analysis. The characteristic chemical shifts of the C-21 and C-22 positions in the ^{1}H and ^{13}C NMR spectra of compounds **9**–**12** (e.g., δ_H 3.30, 3.38/δ_C 49.2 (C-21) and δ_H 3.90, 3.94/δ_C 40.0 (C-22) for **9**) (Tables 8 and 9) suggested that these compounds were congeners of adociaquinones A (**20**) and B (**21**).[5] Notably, **20** and **21** contain a thiomorpholine 1,1-dioxide ring and are regioisomers of each other based on the relative positioning of their nitrogen and sulfur atoms. Comprehensive analysis of 2D NMR spectra of **9**–**12** showed that they contained structures with a pyrrolidine-2,4-diol ring fused to **20** and **21** for **9**/**10** and **11**/**12**, respectively. Chemical shift calculations were conducted for the *cis* and *trans* isomers of **9**/**10** and **11**/**12** (Fig. 7). The results suggested that the

Table 7. ^{1}H and ^{13}C NMR data of **8** in $CDCl_3$

No.	δ_C	δ_H, mult (J in Hz)	HMBC	No.	δ_C	δ_H, mult	HMBC
1	144.9	7.51, s	2, 7, 8	1'	144.9	7.51, s	2', 7', 8'
2	121.5			2'	121.5		
3	16.9	2.63, m 2.85, m	2, 4, 7 2, 4, 5, 7	3'	16.9	2.63, m 2.85, m	
4	18.9	2.14, m 2.25, m	 5	4'	18.9	2.15, m 2.25, m	
5	31.2	1.66, m 2.52, m	4, 6	5'	31.2	1.66, m 2.52, m	
6	37.3			6'	37.3		
7	147.2			7'	147.2		
8	144.1			8'	144.1		
9	170.3			9'	170.2		
10	138.0			10'	138.0		
11	127.6	9.03, s	9, 13, 17, 19	11'	126.9	9.00, s	9', 13', 17', 19'
12	130.5			12'	130.4		
13	182.6			13'	183.5		
14	154.0			14'	134.3	6.84, s	12', 15', 16', 21
15	134.3	6.84, s	13, 14, 17, 21	15'	154.0		
16	184.5			16'	183.6		
17	133.3			17'	133.4		
18	123.0	8.20, s	6, 10, 12, 16	18'	123.8	8.23, s	6', 10', 12', 16'
19	156.3			19'	156.2		
20	32.5	1.50, s	5, 6, 7, 19	20'	32.5	1.50, s	5', 6', 7', 19'
21	31.9	4.73, q (6.9)	13, 14, 15, 22, 14', 15', 16'				
22	17.9	1.48, d (6.9)	14, 21, 15'				

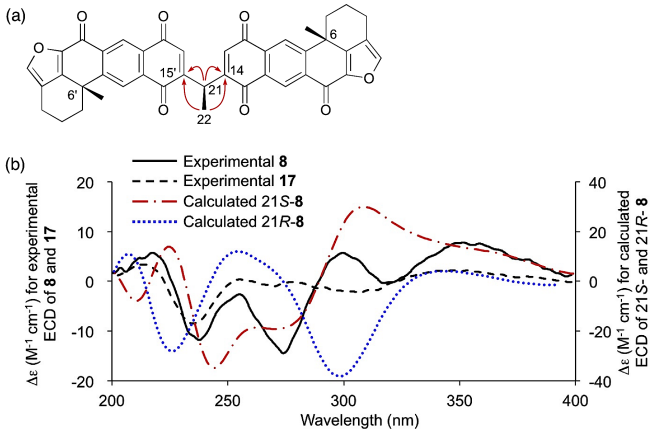

Fig. 6. (a) Key HMBC correlations for **8**. (b) Experimental ECD spectra of **8** and **17** along with calculated ECD spectra of 6*S*,21*S*,6'*S*- and 6*S*,21*R*,6'*S*-**8**.

^{13}C chemical shifts at C-16, C-23, and C-24 for four diastereomers of **9**/**10** and C-13, C-23, and C-24 for four diastereomers of **11**/**12** were clearly different among the *cis* and *trans* configurations in each case. The configurations of 2,4-diol on pyrrolidine ring in **9**–**12** were then all indicated to be *trans*. The 6*S*-configuration was deduced biosynthetically, and a computer simulation of the ECD spectra was performed to determine the absolute configurations of the C-16 and C-23 positions for **9**/**10** and C-13 and C-23 positions for **11**/**12** (Fig. 8). The calculated ECD spectra of (6*S*,16*R*,23*S*)- and (6*S*,16*S*,23*R*)-diastereomers showed the positive and negative Cotton effects observed around 260 and 300 nm (Fig. 8a) and the negative Cotton effect observed around 230 nm (Fig. 8b), respectively, whereas those of (6*S*,13*R*,23*S*)- and (6*S*,13*S*,23*R*)-diastereomers showed the positive Cotton effect observed around 350 nm (Fig. 8c) and the negative Cotton effect observed around 240 nm (Fig. 8d), respectively. Consequently, these characteristic Cotton effects suggested that the configurations of **9**–**12** were indicated to be (6*S*,16*R*,23*S*), (6*S*,16*S*,23*R*), (6*S*,13*R*,23*S*), and (6*S*,13*S*,23*R*), respectively.

Table 8
^{1}H and ^{13}C NMR data of **9** and **10** in DMSO-d_6

	9			**10**		
No.	δ_C	δ_H, mult (*J* in Hz)	HMBC	δ_C	δ_H, mult (*J* in Hz)	HMBC
1	146.0	7.93, s	2, 7, 8	145.5	7.93, s	2, 7, 8
2	121.9			121.5		
3	16.7	2.58, m	2, 7	16.2	2.58, m	2, 7
		2.82, m	2		2.81, m	2
4	18.3	2.06, m		17.8	2.02, m	
		2.19, m			2.20, m	
5	30.9	1.56, m		30.6	1.53, m	
		2.66, m			2.64, m	
6	36.8			36.5		
7	147.7			147.3		
8	143.6			143.1		
9	170.9			170.5		
10	133.4			132.9		
11	125.3	8.66, s	9, 13, 17, 19	124.8	8.65, s	9, 13, 17, 19
12	130.7			130.1		
13	174.1			173.6		
14	104.5			104.0		
15	164.7			164.2		
16	73.2			72.6		
17	143.1			142.7		
18	123.6	7.84, s	6, 10, 12, 16	123.2	1.48, s	6, 10, 12, 16
19	154.8			156.9		
20	32.2	1.44, s	5, 6, 7, 19	31.6	1.48, s	5, 6, 7, 19
21	49.2	3.30, m		48.7	3.31, m	
		3.38, m			3.38, m	
22	40.0	3.90, m	15	39.9	3.90, m	15
		3.94, m				
23	87.9	5.61, m	15	87.4	5.61, m	15
24	44.5	2.11, m	16, 23	44.1	2.00, m	16, 23
		3.24, m	15		3.25, m	15
OH-16		6.76, s	16, 17, 24		6.86, s	16, 17, 24
OH-23		6.96, d (8.8)	23, 24		6.93, d (8.7)	23, 24

Table 9
^{1}H and ^{13}C NMR data of **11** and **12** in DMSO-d_6

	11			**12**		
No.	δ_C	δ_H, mult (*J* in Hz)	HMBC	δ_C	δ_H, mult (*J* in Hz)	HMBC
1	145.7	7.94, s	2, 7, 8	145.4	7.95, s	2, 7, 8
2	121.6			121.6		
3	16.3	2.57, m	2, 5, 7	16.2	2.54, m	2, 5, 7
		2.82, m	2, 5, 7		2.81, m	2, 5, 7
4	17.9	2.08, m		17.8	2.07, m	
		2.21, m			2.23, m	
5	31.9	1.56, m	4, 6	31.1	1.56, m	4, 6
		2.55, m			2.65, m	
6	36.4			36.4		
7	147.7			147.9		
8	143.3			143.4		
9	170.3			170.3		
10	135.2			135.2		
11	124.4	8.17, s	9, 13, 17, 19	122.3	8.16, s	9, 13, 17, 19
12	137.9			137.9		
13	72.4			72.3		
14	164.4			164.5		
15	104.3			104.3		
16	173.5			172.7		
17	134.3			133.9		
18	122.7	8.19, s	6, 10, 12, 16	124.1	8.19, s	6, 10, 12, 16
19	150.9			151.0		
20	31.9	1.47, s	5, 6, 7, 19	31.6	1.43, s	5, 6, 7, 19
21	48.7	3.30, m		48.5	3.33, m	
		3.37, m			3.37, m	
22	40.4	3.87, m	14, 21	39.1	3.96, m	14, 21
		3.95, m	14, 21			
23	87.5	5.61, m	14	87.5	5.61, m	14
24	44.1	2.03, m	13	43.6	2.05, m	13
		3.18, m	13, 14		3.21, m	13, 14
OH-13		6.79, s	12, 13, 14, 24		6.76, s	12, 13, 14, 24
OH-23		7.03, d (8.2)	23, 24		7.07, d (8.0)	23, 24

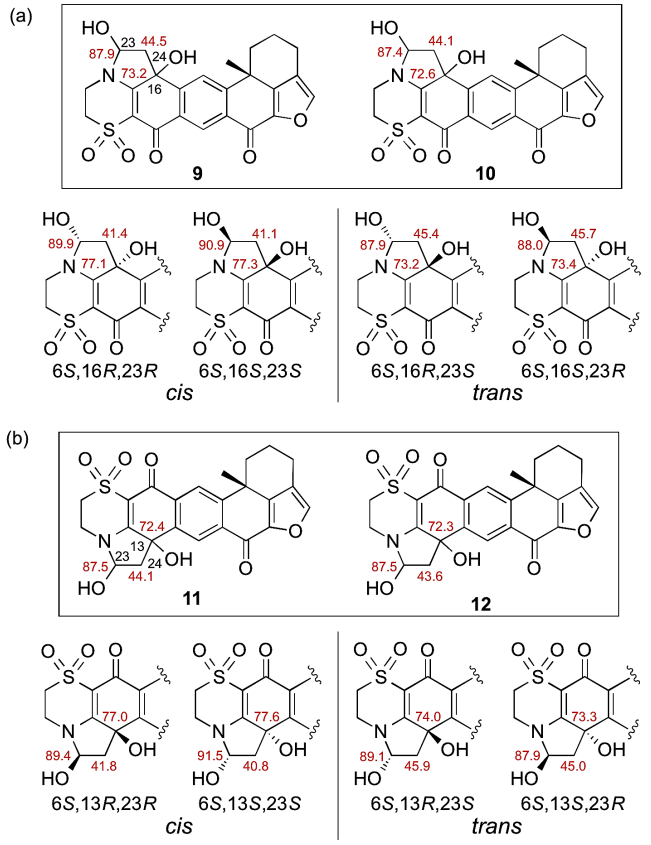

Fig. 7. ^{13}C chemical shifts of **9**–**12** and calculated data for diastereomers of **9**/**10** (a) and **11**/**12** (b).

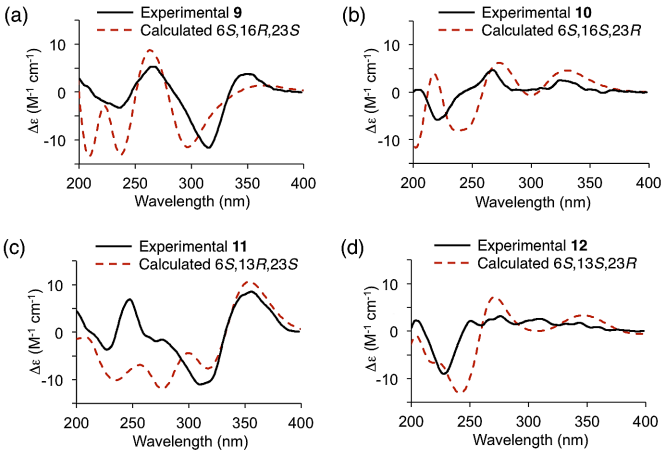

Fig. 8. Experimental ECD spectra of **9**–**12** and calculated ECD spectra of (a) 6*S*,16*R*,23*S*-, (b) 6*S*,16*S*,23*R*-, (c) 6*S*,13*R*,23*S*-, and (d) 6*S*,13*S*,23*R*-diastereomers.

2.1.7. Other xestoquinone derivatives (13-16)

The molecular formula of **13** was determined to be $C_{22}H_{18}O_5$ by HRFABMS, indicating that it contained an extra C_2H_4O unit compared with **17**. The NMR spectra of **13** (Table 10) revealed the presence of a hydroxyethyl group, as well as a quaternary carbon. Interestingly, however, these data revealed the absence of an sp^2 methine. Consideration of the 2D NMR spectra of **13** confirmed it to be 1-(2-hydroxyethyl)xestoquinone. The NMR and FABMS data collected for the inseparable mixture of **14** and **15** (1:1, mol/mol) were consistent with these materials being a mixture of C-21 epimers of 1-(1-hydroxyethyl)xestoquinone. The carbon chemical shifts of the epimers were the same except for C-2, C-21, and C-22 (Table 10). Compound **16** was revealed to be 3-hydroxyxestoquinone based on its coupling constant (5.2 Hz) between H-3 and H-4β (δ 2.55) (Table 11, Fig. 9), which indicated that H-3 and OH-3 were pseudoequatorial and pseudoaxial, respectively. Thus, **16** existed in a 3*S* configuration.[6]

Table 10
^{1}H and ^{13}C NMR data of **13** and a mixture of **14** and **15** in $CDCl_3$

	13			A mixture of **14** and **15**		
No.	δ_C	δ_H, mult (*J* in Hz)	HMBC	δ_C	δ_H, mult (*J* in Hz)	HMBC
1	157.5			159.2		
2	118.8			117.1, 117.2		
3	17.2	2.64, m 2.81, m	2, 4, 7 2	17.7	2.66, m 2.85, m	2, 4, 7 2, 4, 7
4	18.5	2.30, m 2.19, m		18.5	2.24, m 2.18, m	
5	30.9	1.75, m 2.50, m	6	31.0	1.72, m 2.53, m	
6	37.4			37.4		
7	149.4			148.6		
8	142.5			142.5		
9	169.1			169.9		
10	138.0			137.9		
11	126.7	8.83, s	9, 11, 17, 19	126.0	8.98, s	9, 11, 17, 19
12	130.1			130.3		
13	183.7			183.8		
14	139.4	6.99, d (10.4)	12, 16	139.4	7.01, d (10.4)	12, 16
15	138.5	6.98, d (10.4)	13, 17	138.6	7.02, d (10.4)	12, 16
16	184.7			184.7		
17	132.8			133.1		
18	123.0	8.10, s	6, 10, 12, 16	123.1	8.18, s	6, 10, 12, 16
19	156.1			156.1		
20	32.6	1.46, s	5, 6, 7, 19	32.6	1.49, s	5, 6, 7, 19
21	31.2	3.00, m	1, 2, 22	64.0, 64.2	5.01, q (6.8)	1, 2, 22
22	60.2	4.02, m 4.10, m	1 1	21.4, 21.5	1.62, d (6.8)	1, 21

Table 11
^{1}H and ^{13}C NMR data of **16** in $CDCl_3$

No.	δ_C	δ_H, mult (*J* in Hz)	HMBC
1	147.0	7.84, s	2, 7, 8
2	125.6		
3	59.8	5.10, d (5.2)	2
4	29.7	2.18, br d (15.2) 2.55, dddd (15.2, 13.4, 5.2, 3.9)	6
5	27.5	2.06, td (13.4, 3.9) 2.46, dt (13.4, 3.9)	4, 20 3, 7
6	37.2		
7	145.7		
8	144.1		
9	170.5		
10	144.1		
11	127.2	9.01, s	9, 11, 17, 19
12	130.5		
13	183.7		
14	139.4	7.04, d (10.4)	12, 16
15	138.7	7.03, d (10.4)	13, 17
16	184.6		
17	133.4		
18	123.2	8.22, s	6, 10, 12, 16
19	155.7		
20	32.5	1.47, s	5, 6, 7, 19

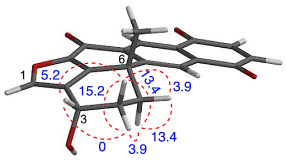

Fig. 9. Coupling constants (Hz) for **16**.

2.2. Possible biosynthetic pathway

We have proposed plausible biogenetic pathways for the preparation of **1**, **3**, **4**, and **7** from xestoquinone (**17**) and its derivatives xestoquinol[7] (**22**) and xestoquinol sulfate (**18**), which are shown in Scheme 1. A coupling reaction between the quinone and quinol moieties in **17** and **22** would afford dimer **7**, followed by the formation of trimer **1** (Scheme 1a). Dimer **6** and trimer **2** would be biosynthesized in the same way. Alternatively, the addition of water to **18** would be lead to the formation of **23**, which would undergo a coupling reaction with **17** to afford the cationic species **24**. Cation **24** would then undergo an etherification reaction with the oxygen atom at C-13 to give **4** (Scheme 1b). Alternatively, cation **24** could undergo a Baeyer–Villiger oxidation, followed by a stereoselective lactonization reaction to yield **3** (Scheme 1b).

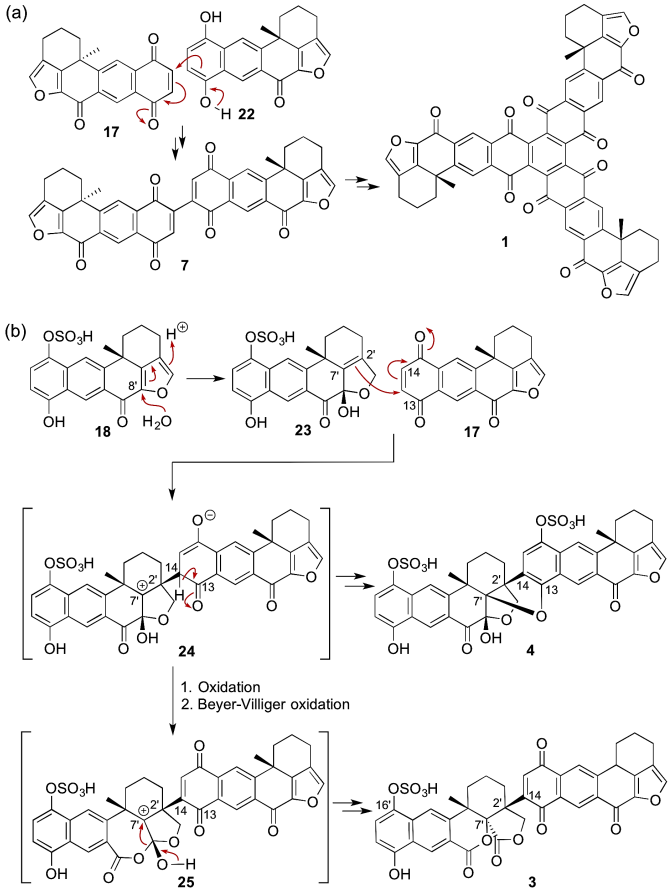

Scheme 1. Possible biosynthetic pathway for the preparation of **1**, **3**, **4**, and **7** from **17**.

3. Biological studies

Among compounds isolated in this study, **1**–**3**, **5**–**8**, **13**, **17**, and **19** showed potent inhibitory activities against USP7 with IC_{50} values in the range of 0.13–2.0 μM (Table 12; **14**–**16** and **18** were not tested). Since USP7 is a member of the cysteine protease family, it is possible that the inhibitory activities of these compounds, with the exception of **1** and **2**, could be attributed to the reaction of their quinone moieties (C-14 or C-15) with the catalytic sulfhydryl group positioned in the active site of USP7. Previously, Copp et al. demonstrated that *N*-acetyl-L-cysteine reacted at the vacant quinone positions C-14 and C-15 of halenaquinone.[8] Given that the C-14 and C-15 positions of compounds **1** and **2** are connected to other structural units, these two compounds must exhibit their inhibitory activity via some other unknown mechanism.

Table 12
USP7 inhibitory activities of **1**–**13**, **17**, and **19**

Compounds	IC_{50} (μM)	Compounds	IC_{50} (μM)
1	0.75	**9**	>5.0 [a]
2	0.36	**10**	>5.0 [a]
3	2.0	**11**	>5.0 [a]
4	>5.0 [a]	**12**	>5.0 [a]
5	1.2	**13**	1.4
6	0.35	**17**	0.13
7	0.47	**19**	1.3
8	0.49		

[a] The inhibitory ratios (%) of **4** and **9**–**12** at 5 μM were 14, 20, 17, 14, and 12%, respectively.

4. Conclusions

The xestoquinone derivatives described in this study are structurally unprecedented. To the best of our knowledge, only four *cyclo*-tri-1,4-naphthoquinone derivatives have been reported to date,[9] highlighting the structural novelty of **1** and **2**, which are composed of three pentacyclic xestoquinone (**17**) units. Moreover, only two halenaquinol dimers, including dihalenaquinolides A and B,[10] have been isolated to date from natural sources. In these two compounds, the halenaquinol (**19**) units are joined together by a single peroxide bond between the oxygen atoms of their respective quinol moieties. In contrast, the monomeric units in **5**–**7** were joined together through a single C–C bond between their respective quinone/quinol moieties to give a "tail-to-tail" linkage, whereas **3** and **4** were joined through "head-to-tail" linkages. Furthermore, a large number of compounds containing γ- and/or δ-lactone rings have been isolated from natural sources and synthesized. It is noteworthy however, that **3** was the first reported example of a natural product containing two lactone rings sharing a single carbon atom. The structure of **4** was determined to be unique compared with the other compounds isolated in this study because it contained an ether bond between the quinol group at C-13 and the quaternary carbon at C-7', as well as a C–C bond between C-14 and C-2'. Compounds **9**–**12** contained new carbon frameworks composed of xestoquinone, thiomorpholine 1,1-dioxide, and pyrrolidine-2,4-diol moieties, and also existed as regio- and/or stereoisomers of each other. Studies towards the mechanisms of USP7 inhibitory activities of **1** and **2** are currently under way.

5. Experimental

5.1. General experimental procedures

Optical rotations were measured on a JASCO DIP-1000 polarimeter (Jasco, Tokyo, Japan) in CH_3CN or MeOH. UV spectra were measured on a JASCO V-550. Electronic circular dichroism (ECD) spectra were measured on a JASCO J-820 spectropolarimeter in CH_3CN or MeOH. IR spectra were recorded on a Perkin Elmer Frontier FT-IR spectrophotometer (Perkin Elmer, Waltham, USA). ^1H and ^{13}C NMR spectra were recorded on a JEOL JNM-ECX400, Bruker Avance 500 or Bruker Avance 600 NMR spectrometer (Bruker, Billerica, USA) in $CDCl_3$ or DMSO-d_6. Chemical shifts (δ) were measured in ppm relative to the residual solvent peaks (i.e., δ_H 7.24 and δ_C 77.0 for $CDCl_3$ or δ_H 2.49 and δ_C 39.5 for DMSO-d_6). ESIMS analyses were measured on a Bruker Bio-TOF mass spectrometer. FABMS analyses were conducted on a JEOL JMS-700 MStation mass spectrometer (JEOL, Tokyo, Japan).

5.2. Extraction and isolation of the compounds from the animal material

The sponge *Petrosia alfiani* (300 g, wet weight) was collected at a depth of 10 m in Ti Toi (North Sulawesi, Indonesia) in December 2006 and immediately soaked in EtOH. A voucher specimen (RMNH POR. 8525) of this material was deposited at the Naturalis Biodiversity Center in The Netherlands. The sponge was extracted with EtOH, and the resulting extract was evaporated under vacuum to give an aqueous residue, which was extracted with EtOAc. The EtOAc fraction was partitioned between *n*-hexane and 90% MeOH-H_2O. The 90% MeOH-H_2O fraction (1.4 g) was subjected to column chromatography over silica gel eluting with a mixture of *n*-hexane and EtOAc (2:1 and 1:1, v/v (Fr. A)), followed by a mixture of $CHCl_3$ and MeOH (9:1 (Frs. B–D) and 1:1, v/v). Fr. A (400 mg) was determined to be xestoquinone (**17**). Frs. B and D (120 mg) were combined and purified by preparative HPLC [YMC-Pack R&D D-SIL-5 column (20 × 250 mm), a linear gradient elution from *n*-hexane/$CHCl_3$ (1:1, v/v) to $CHCl_3$ over 90 min; Inertsil Diol column (20 × 250 mm), isocratic *n*-hexane/$CHCl_3$ (1:1, v/v)] to yield petroquinones F (**6**, 4.2 mg) and G (**7**, 3.6 mg). Fr. C (930 mg) was purified by column chromatography over silica gel eluting with a 40:1 (v/v) mixture of $CHCl_3$/MeOH to give Frs. C1–C3. Fr. C1 (20 mg) was purified by preparative HPLC [YMC-Pack R&D D-SIL-5 column (20 × 250 mm) with linear gradient elution from *n*-hexane/$CHCl_3$ (1:2, v/v) to $CHCl_3$ over 90 min] to yield petroquinones A (**1**, 0.14 mg), B (**2**, 2.5 mg), and H (**8**, 1.3 mg). Fr. C2 (1.0 g) was repeatedly purified by column chromatography over silica gel eluting with $CHCl_3$ followed by a 1:1 (v/v) mixture of *n*-hexane/EtOAc. The crude material was subsequently purified by preparative HPLC [LiChrosorb SI-60 column (20 × 250 mm) with linear gradient elution from CH_2Cl_2 to CH_2Cl_2/MeOH (70:1) over 90 min] to afford Frs. C2-1, C2-2, and C2-3. Fr. C2-1 (13 mg) was purified by preparative HPLC [COSMOSIL 5SL-II column (20 × 250 mm) eluting with CH_2Cl_2/MeOH (99:1, v/v)] to yield a C-21 epimeric mixture of 1-(1-hydroxyethyl)xestoquinone (**14** and **15**, 5.9 mg). Fr. C2-2 (17 mg) was purified by preparative HPLC [Inertsil Diol column (20 × 250 mm) eluting with *n*-hexane/$CHCl_3$ (2:1, v/v)] to yield 3*S*-3-hydroxyxestoquinone (**16**, 3.8 mg). Fr. C2-3 (15 mg) was purified by preparative HPLC [COSMOSIL 5SL-II column (20 × 250 mm) eluting with CH_2Cl_2/MeOH (99:1, v/v)] to give 1-(2-hydroxyethyl)xestoquinone (**13**, 6.1 mg).

The sponge *P. alfiani* (700 g, wet weight) was collected at a depth of 10 m in Budo (North Sulawesi, Indonesia) in September 2008 and immediately soaked in EtOH. A voucher specimen (RMNH POR. 8522) of this material was deposited at the Naturalis Biodiversity Center in The Netherlands. The sponge was extracted with EtOH, and the resulting extract was evaporated under vacuum to give an aqueous residue, which was extracted with EtOAc. The EtOAc fraction (4.3 g) was then purified by column chromatography over silica gel eluting with $CHCl_3$/MeOH (98:2, 97:3, 95:1, and 9:1, v/v), followed by MeOH. The fraction eluted with $CHCl_3$/MeOH (97:3, v/v) (18 mg) was determined to be xestoquinone (**17**). The fraction eluted with MeOH (211 mg) was purified by column chromatography over silica gel eluting with CH_2Cl_2/MeOH (20:1 and 9:1, v/v). The fraction (57 mg) eluted with CH_2Cl_2/MeOH (20:1, v/v) was purified by preparative HPLC [Develosil C30-UG-5 column (20 × 250 mm) eluting with 25% CH_3CN-H_2O] to yield petroquinones I (**9**, 2.7 mg) and J (**10**, 8.3 mg). The fraction (64 mg) eluted with CH_2Cl_2/MeOH (9:1, v/v) was purified by preparative HPLC [Develosil C30-UG-5 column (20 × 250 mm) eluting with CH_3CN/H_2O (1:3, v/v)] to yield petroquinones K (**11**, 0.5 mg) and L (**12**, 2.8 mg).

The H_2O fractions obtained from the two sponges described above were combined and extracted with *n*-BuOH. The *n*-BuOH fraction (6.8 g) was then purified by ODS column chromatography eluting with MeOH/H_2O (3:2, v/v), followed by purification by column chromatography over silica gel (CH_2Cl_2/MeOH (9:1 and 8:2, v/v) then CH_2Cl_2/MeOH/H_2O (6:4:1, v/v/v). The fraction eluted with CH_2Cl_2/MeOH (9:1, v/v) (14 mg) was purified by preparative HPLC [Asahipak GS-310P column (21.5 × 500 mm) eluting with CH_2Cl_2/MeOH/H_2O (6:4:1, v/v/v)] to yield petroquinone E (**5**, 1.7 mg). The fraction eluted with CH_2Cl_2/MeOH (8:2, v/v) (25 mg) was purified by preparative HPLC [Asahipak GS-310P column (21.5 × 500 mm) eluting with CH_2Cl_2/MeOH/H_2O (6:4:1, v/v/v); Develosil C30-

UG-5 column (20 × 250 mm) eluting with CH_3CN/H_2O (7:13 and 1:1, v/v)] to yield petroquinone C (**3**, 2.9 mg). The fraction eluted with $CH_2Cl_2/MeOH/H_2O$ (6:4:1, v/v/v) (39 mg) was purified by preparative HPLC [Asahipak GS-310P column (21.5 × 500 mm), $CH_2Cl_2/MeOH/H_2O$ (6:4:1, v/v/v); Develosil C30-UG-5 column (20 × 250 mm), CH_3CN/H_2O (1:4, v/v)] to yield petroquinone D (**4**, 0.72 mg).

5.3. Petroquinone A (1)

$[\alpha]_D^{20}$ +389 (*c* 0.10, CH_3CN); UV (CH_3CN) λ_{max} (log ε) 296 (5.1), 262 (5.1), 220 (5.1) nm; ECD (100 μM, CH_3CN) λ_{max} (Δε) 225 (sh, 7.9), 252 (sh, 4.4), 275 (–24.0), 307 (–9.0) nm (Fig. 2b); IR (film) ν_{max} 2925, 1672, 1446, 1375, 1286, 1214, 1042 cm^{-1}; NMR data ($CDCl_3$), see Table 1; HRESITOFMS *m/z* 971.2109 $[M+Na]^+$ (calcd for $C_{60}H_{36}O_{12}Na$, 971.2099), 1919.4331 $[2M+Na]^+$ (calcd for $C_{60}H_{36}O_{12}Na$, 1919.4306).

5.4. Petroquinone B (2)

$[\alpha]_D^{20}$ –6.0 (*c* 0.10, CH_3CN); UV (CH_3CN) λ_{max} (log ε) 294 (5.0), 264 (5.0), 224 (4.9) nm; ECD (100 μM, CH_3CN) λ_{max} (Δε) 237 (–8.1), 260 (–0.3), 274 (–2.5), 290 (1.9), 316 (–2.4) nm (Fig. 2b); IR (film) ν_{max} 2924, 1671, 1445, 1284, 1214, 1047, 1149 cm^{-1}; NMR data ($CDCl_3$), see Table 2; HRESITOFMS *m/z* 949.2275 $[M+H]^+$ (calcd for $C_{60}H_{37}O_{12}$, 949.2280), 971.2103 $[M+Na]^+$ (calcd for $C_{60}H_{36}O_{12}Na$, 971.2099).

5.5. Petroquinone C (3)

$[\alpha]_D^{20}$ –57 (*c* 0.78, MeOH); UV (MeOH) λ_{max} (log ε) 300 (3.9), 266 (4.3), 220 (4.4) nm; ECD (100 μM, MeOH) λ_{max} (Δε) 224 (–23.4), 245 (–2.2), 268 (–15.3) nm; IR (film) ν_{max} 3424, 2923, 1780, 1736, 1664, 1445, 1341, 1203, 1149, 1045, 816 cm^{-1}; NMR data (DMSO-d_6), see Table 3; HRFABMS *m/z* 749.1364 $[M–H]^–$ (calcd for $C_{40}H_{29}O_{13}S$, 749.1334).

5.6. Petroquinone D (4)

$[\alpha]_D^{20}$ +36 (*c* 0.36, MeOH); UV (MeOH) λ_{max} (log ε) 312 (4.5), 274 (4.9), 226 (5.0), 202 (4.8) nm; ECD (100 μM, MeOH) λ_{max} (Δε) 223 (21.2), 242 (–43.6), 277 (50.5), 311 (–5.6) nm; IR (film) ν_{max} 3380, 2925, 1626, 1445, 1340, 1232, 1149, 1030, 809 cm^{-1}; NMR data (DMSO-d_6), see Table 4; ESIMS *m/z* 407.1 $[M – 2H]^{2–}$, 815.0 $[M–H]^–$; HRESIMS *m/z* 407.0531 $[M–2H]^{2–}$ (calcd for $C_{40}H_{30}O_{15}S_2$, 407.0500).

5.7. Petroquinone E (5)

$[\alpha]_D^{20}$ +27 (*c* 0.23, MeOH); UV (MeOH) λ_{max} (log ε) 302 (4.3), 262 (4.3), 224 (4.4), 204 (4.5) nm; ECD (500 μM, MeOH) λ_{max} (Δε) 206 (–0.1), 219 (2.1), 242 (–5.0), 284 (0.0), 308 (–1.3) nm; IR (film) ν_{max} 3261, 2924, 2854, 1660, 1444, 1215, 1037, 587 cm^{-1}; NMR data (DMSO-d_6), see Table 5; HRFABMS *m/z* 715.1310 $[M–H]^–$ (calcd for $C_{40}H_{27}O_{11}S$, 715.1280).

5.8. Petroquinone F (6)

$[\alpha]_D^{26}$ +23 (*c* 0.10, CH_3CN); UV (CH_3CN) λ_{max} (log ε) 296 (5.2), 272 (5.2), 222 (5.3), 198 (5.2) nm; ECD (100 μM, CH_3CN) λ_{max} (Δε) 204 (0.8), 218 (2.6), 239 (–4.2), 298 (1.3), 318 (–1.1), 361 (2.1) nm; IR (film) ν_{max} 2922, 1667, 1445, 1288, 1215, 1150, 1041, 436 cm^{-1}; NMR data ($CDCl_3$), see Table 6; HRESIMS *m/z* 635.1651 $[M+H]^+$ (calcd for $C_{40}H_{27}O_8$, 635.1700), 657.1526 $[M+Na]^+$ (calcd for $C_{40}H_{26}O_8Na$, 657.1520).

5.9. Petroquinone G (7)

$[\alpha]_D^{26}$ +26 (*c* 0.10, CH_3CN); UV (CH_3CN) λ_{max} (log ε) 296 (5.4), 272 (5.5), 222 (5.5), 202 (5.4) nm; ECD (100 μM, CH_3CN) λ_{max} (Δε) 207 (3.3), 216 (8.1), 238 (–14.7), 301 (1.5), 323 (–3.0), 362 (4.7) nm; IR (film) ν_{max} 2925, 1663, 1444, 1320, 1287, 1217, 1149, 1040, 435 cm^{-1}; NMR data ($CDCl_3$), see Table 6; HRESIMS *m/z* 635.1665 $[M+H]^+$ (calcd for $C_{40}H_{27}O_8$, 635.1700), 657.1546 $[M+Na]^+$ (calcd for $C_{40}H_{26}O_8Na$, 657.1526).

5.10. Petroquinone H (8)

$[\alpha]_D^{26}$ +82 (*c* 0.10, CH_3CN); UV (CH_3CN) λ_{max} (log ε) 264 (5.2), 218 (5.2), 202 (5.2) nm; ECD (100 μM, CH_3CN) λ_{max} (Δε) 201 (1.3), 219 (5.9), 239 (–12.1), 255 (–2.5), 275 (–14.6), 301 (5.8), 318 (–0.5), 352 (7.9) nm (Fig. 6b); IR (film) ν_{max} 2937, 1664, 1300, 1215, 1152, 1040, 928, 439 cm^{-1}; NMR data ($CDCl_3$), see Table 7; HRESIMS *m/z* 663.2049 $[M+H]^+$ (calcd for $C_{42}H_{31}O_8$, 663.2013).

5.11. Petroquinone I (9)

$[\alpha]_D^{20}$ –35 (*c* 0.20, CH_3CN); UV (CH_3CN) λ_{max} (log ε) 314 (4.6), 244 (4.7) nm; ECD (200 μM, CH_3CN) λ_{max} (Δε) 238 (–3.3), 268 (5.3), 317 (–11.7), 351 (3.8) nm (Fig. 8a); IR (film) ν_{max} 3264, 2928, 1667, 1607, 1350, 1607, 1281, 1125, 1043 cm^{-1}; NMR data (DMSO-d_6), see Table 8; HRFABMS *m/z* 468.1112 $[M+H]^+$ (calcd for $C_{24}H_{22}NO_7S$, 468.1117).

5.12. Petroquinone J (10)

$[\alpha]_D^{20}$ +10 (*c* 0.20, CH_3CN); UV (CH_3CN) λ_{max} (log ε) 314 (4.9), 242 (5.1) nm; ECD (200 μM, CH_3CN) λ_{max} (Δε) 221 (–5.9), 268 (4.7), 325 (2.5) nm (Fig. 8b); IR (film) ν_{max} 3201, 2927, 1667, 1608, 1350, 1607, 1282, 1125, 1043 cm^{-1}; NMR data (DMSO-d_6), see Table 8; HRFABMS *m/z* 468.1121 $[M+H]^+$ (calcd for $C_{24}H_{22}NO_7S$, 468.1117).

5.13. Petroquinone K (11)

$[\alpha]_D^{27}$ +30 (*c* 0.20, CH_3CN); UV (CH_3CN) λ_{max} (log ε) 344 (4.9), 316 (5.0), 264 (5.0), 234 (5.1), 204 (5.2) nm; ECD (200 μM, CH_3CN) λ_{max} (Δε) 248 (6.9), 310 (–11.0) nm (Fig. 8c); IR (film) ν_{max} 3348, 2926, 1665, 1609, 1282, 1123, 1050 cm^{-1}; NMR data (DMSO-d_6), see Table 9; HRFABMS *m/z* 468.1129 $[M+H]^+$ (calcd for $C_{24}H_{22}NO_7S$, 468.1117).

5.14. Petroquinone L (12)

$[\alpha]_D^{27}$ +19 (*c* 0.20, CH_3CN); UV (CH_3CN) λ_{max} (log ε) 342 (4.7), 316 (4.7), 258 (4.8), 232 (4.9) nm; ECD (200 μM, CH_3CN) λ_{max} (Δε) 204 (2.3), 228 (–9.0) nm (Fig. 8d); IR (film) ν_{max} 3348, 2926, 1665, 1609, 1282, 1123, 1050 cm^{-1}; NMR data (DMSO-d_6), see Table 9; HRFABMS *m/z* 468.1131 $[M+H]^+$ (calcd for $C_{24}H_{22}NO_7S$, 468.1117).

5.15. 1-(2-Hydroxyethyl)xestoquinone (13)

$[\alpha]_D^{25}$ –19 (*c* 0.50, CH_3CN); UV (CH_3CN) λ_{max} (log ε) 312 (5.0), 262 (5.0), 254 (5.1), 220 (5.1) nm; ECD (100 μM, CH_3CN) λ_{max} (Δε) 215 (4.3), 241 (–4.5), 266 (0.9), 318 (–2.5) nm; IR (film) ν_{max} 3037, 2944, 1655, 1603, 1479, 1464, 1319, 1222, 1134, 1056, 846, 425 cm^{-1}; NMR data ($CDCl_3$), see Table 10; HRFABMS *m/z* 363.1277 $[M+H]^+$ (calcd for $C_{22}H_{19}O_5$, 363.1233).

5.16. A C-21 epimeric mixture of 1-(1-hydroxyethyl)-xestoquinone (14 and 15)

NMR data ($CDCl_3$), see Table 10; HRFABMS *m/z* 363.1273 $[M+H]^+$ (calcd for $C_{22}H_{19}O_5$, 363.1233).

5.17. 3*S*-3-Hydroxyxestoquinone (16)

$[\alpha]_D^{20}$ –23 (*c* 0.10, CH_3CN); UV (CH_3CN) λ_{max} (log ε) 292 (4.8), 260 (4.9), 254 (4.9), 216 (4.9) nm; ECD (100 μM, CH_3CN) λ_{max} (Δε) 234 (–6.0), 255 (–1.7), 278 (–2.9), 356 (0.2) nm; IR (film) ν_{max} 3388, 2925, 2854, 1669, 1602, 1456, 1440, 1320, 1259, 1136, 1024, 846, 794 cm^{-1}; NMR data ($CDCl_3$), see Table

11; HRESIMS *m/z* 357.0729 $[M+Na]^+$ (calcd for $C_{20}H_{14}NaO_5$, 357.0739).

5.18. Preparation of 6 from 17

To a solution of **17** (9.8 mg) in 1,2-dichloroethane (30 μL) was added quinoline (0.82 mg) and acetic acid (5 μL), and the resulting mixture was stirred at 60 °C for 16 h. The mixture was then cooled to room temperature and concentrated *in vacuo* to give a residue, which was purified by preparative HPLC over a YMC-Pack R&D D-SIL-5 column (20 × 250 mm) eluting with a 2:1 (v/v) mixture of *n*-hexane and CH_2Cl_2 to yield **6** (0.67 mg) and **17** (3.23 mg).

5.19. Conformational analyses for 1, 3, 4, 8–12, and 16 and chemical shift calculations for 4 and 9–12

All of the conformational searches conducted in the current study were performed with version 1.1.8 of the Spartan'14 software (Wavefunction Inc., Irvine, CA, USA) using a commercially available PC (operating system, Windows 7 Professional SP1 64-bit; CPU, QuadCore Core i7-3770 processor 3.40 GHz; RAM, 8 GB). Stable conformers up to 10 kcal/mol for **1**; **3**; 8'*R*- and 8'*S*-**4**; 6*S*,21*R*,6'*S*-, and 6*S*,21*S*,6'*S*-**8**; 6*S*,16*R*,23*R*-, 6*S*,16*S*,23*S*-, 6*S*,16*R*,23*S*-, and 6*S*,16*S*,23*R*-**9**/**10**; 6*S*,13*R*,23*R*-, 6*S*,13*S*,23*S*-, 6*S*,13*R*,23*S*-, and 6*S*,13*S*,23*R*-**11**/**12**; and **16** were initially searched using the Merck molecular force field (MMFF) method.[11] The top 100 most stable conformers obtained in this way were further optimized using the Hartree–Fock (HF) method with 3-21G. The resulting conformers were subjected to conformational analyses and chemical shift calculations using DFT with EDF2/6-31G* (Figs. 4c and 7).

5.20. ECD calculations for 8–12

Conformers of >0.1% suggested above were subsequently optimized using density functional theory (DFT) with B3LYP/6-31G*. All of the ECD calculations were conducted with Gaussian09 (Revision D.01 by Gaussian, Wallingford, CT, USA)[12] on a PC (Operating System, CentOS a Linux; CPU, Intel Xeon E5-2603 v3 processors 1.60 GHz; RAM, 32 GB). For the ECD calculations involving the diastereomers of 8–12, we selected the dominant conformers capable of covering >99% of the population from the Boltzmann's law. Time-dependent density functional theory (TDDFT) calculations were conducted at the B3LYP/6-31G* level for these conformers. The resulting rotational strength data were converted to Gaussian curves (bandwidth sigma = 3000 cm^{-1}) to obtain the ECD spectra of the different conformers. No wavelength correction was used in this process because the corresponding electronic transitions successfully reproduced the UV absorbance peaks and the diagnostic ECD peaks were also reasonably reproduced. These spectra were then correctively summed to give the corresponding theoretical ECD spectrum (Figs. 6b and 8). To evaluate the accuracy of this process, we also conducted TDDFT calculations using the CAM-B3LYP functional, according to the procedure described above. Pleasingly, these calculations resulted in the same assignment of the configuration.

5.21. Measurement of the USP7 inhibitory activity

The inhibitory activities of the compounds towards USP7 were measured using recombinant USP7 (LifeSensors, Inc., Malvern, USA) with ubiquitin-Rh110 (LifeSensors, Inc.) as a quenched, fluorescent substrate in 96-well plates. USP7 (0.9 nM) was incubated with a test sample at 25 °C for 30 min in 80 μL of 20 mM Tris-HCl buffer (pH 8.0) containing 2 mM $CaCl_2$, 0.05% CHAPS, and 2 mM 2-mercaptoethanol. Each well was then treated with 0.5 □M ubiquitin-Rh110 in 20 μL of the buffer, and the resulting mixture was incubated at 25 °C for 180 min. The fluorescence intensity due to rhodamine, produced by the USP7-catalyzed cleavage of the amide bond between the C-terminal glycine of ubiquitin and the rhodamine moiety in ubiquitin-Rh110, was measured within the linear range of the assay on a fluorometric plate reader with excitation and emission wavelengths of 490 and 530 nm, respectively.

Acknowledgments

We thank Prof. M. Namikoshi and Dr. K. Ukai of Tohoku Pharmaceutical Univrsity, Dr. H. Kobayashi of the University of Tokyo, and Dr. H. Rotinsulu of Universitas Pembangunan for collecting the sponges, F. Losung of Sam Ratulangi University for her technical assistance, and Dr. S. Ando of Kumamoto University for his valuable advise on the conversion of **17** to **6**. This work was financially supported by Grants for Scientific Research (Nos. 18406002, 25293025, 26305005) from MEXT (Japan).

References and notes

1. Nakamura, H.; Kobayashi, J.; Kobayashi, M.; Ohizumi, Y.; Hirata, Y. *Chem. Lett.* **1985**, *14*, 713–716.
2. Blunt, J. W.; Copp, B. R.; Keyzers, R. A.; Munro, M. H. G.; Prinsep, M. R. *Nat. Prod. Rep.* **2016**, *32*, 116–211.
3. Colland, F. *Biochem. Soc. Trans.* **2010**, *38*, 137–143.
4. Nicholson, B.; Suresh Kumar, K. G. *Cell Biochem. Biophys*. **2011**, *60*, 61–68.
5. Schmitz, F. J.; Bloor, S. J. *J. Org. Chem.* **1988**, *53*, 3922–3925.
6. 3*R*-3-Hydroxyxestoquinone has been prepared from halenaquinol. Nakamura, M.; Kakuda, T.; Oba, Y.; Ojika, M.; Nakamura, H. *Bioorg. Med. Chem*. **2003**, *11*, 3077–3082.
7. Although xestoquinol (**22**) has not yet been isolated as a natural product, it was converted from xestoquinone (**17**). Harada, N.; Sugioka, T.; Uda, H.; Kuriki, T. *J. Org. Chem.* **1990**, *55*, 3158–3163.
8. Wang, J.; Bourguet-Kondracki, M.-L.; Longeon, A.; Dubois, J.; Valentin, A.; Copp, B. R. *Bioorg. Med. Chem. Lett.* **2011**, *21*, 1261–1264.
9. (a) Sidhu, G. S.; Prasad, K. K. *Tetrahedron Lett.* **1970**, 1739–1742; (b) Khan, M. R.; Timi, D. *Fitoterapia* **1999**, *70*, 320–321; (c) Hirakawa, K.; Ogiue, E.; Motoyoshiya, J.; Yajima, M. Phytochemistry **1986**, *25*, 1494–1495; (d) Cooke, R. G.; Down, J. G. *Tetrahedron Lett.* **1970**, 583–584.
10. Shen, Y. C.; Prakash, C. V. S.; Guh, J.-H. *Tetrahedron Lett.* **2004**, *45*, 2463–2466.
11. Halgren, T. A. *J. Comp. Chem.* **1996**, *17*, 490–641.
12. Frisch, M. J.; Trucks, G. W.; Schlegel, H. B.; Scuseria, G. E.; Robb, M. A.; Cheeseman, J. R.; Scalmani, G.; Barone, V.; Mennucci, B.; Petersson, G. A.; Nakatsuji, H.; Caricato, M.; Li, X.; Hratchian, H. P.; Izmaylov, A. F.; Bloino, J.; Zheng, G.; Sonnenberg, J. L.; Hada, M.; Ehara, M.; Toyota, K.; Fukuda, R.; Hasegawa, J.; Ishida, M.; Nakajima, T.; Honda, Y.; Kitao, O.; Nakai, H.; Vreven, T.; Montgomery, Jr., J. A.; Peralta, J. E.; Ogliaro, F.; Bearpark, M.; Heyd, J. J.; Brothers, E.; Kudin, K. N.; Staroverov, V. N.; Kobayashi, R.; Normand, J.; Raghavachari, K.; Rendell, A.; Burant, J. C.; Iyengar, S. S.; Tomasi, J.; Cossi, M.; Rega, N.; Millam, J. M.; Klene, M.; Knox, J. E.; Cross, J. B.; Bakken, V.; Adamo, C.; Jaramillo, J.; Gomperts, R.; R. E. Stratmann, R. E.; Yazyev, O.; Austin, A. J.; Cammi, R.; Pomelli, C.; Ochterski, J. W.; Martin, R. L.; Morokuma, K.; Zakrzewski, V. G.; Voth, G. A.; Salvador, P.; Dannenberg, J. J.; Dapprich, S.; Daniels, A. D.; Farkas, Ö.; Foresman, J. B.; Ortiz, J. V.; Cioslowski, J.; Fox, D. J. *Gaussian 09, Revision A.02*, 2009, Gaussian, Inc., Wallingford CT.